USING A THERMALHYDRAULICS SYSTEM CODE TO ESTIMATE HEAT TRANSFER COEFFICIENTS FOR A CRITICAL HEAT FLUX EXPERIMENT

B.A. Statham
McMaster University, Ontario, Canada

Abstract

RELAP5/SCDAPSIM MOD 3.4 is used to predict wall temperature before and after critical heat flux (CHF) is reached in a vertical, uniformly heated tube using light water as the working fluid. The heated test section is modeled as a 1 m long Inconel 600 tube having an OD of 6.35 mm and ID of 4.57 mm with a 0.5 m long unheated development length at the inlet. Simulations are performed at pressures of 0.5 to 2.0 MPa with mass fluxes from 500 to 2000 kg m^{-2} s^{-1} and inlet qualities ranging from -0.2 to 0. Loss of flow simulations are performed with flow reduction rates of 10, 20, 50, and 100 kg m^{-2} s^{-2}. Inlet mass flux at CHF was nominally independent of rate in the model; this may or may not be realistic.

1. Introduction

Convective boiling heat transfer is an important consideration in the operation of a wide variety of industrial process systems. It is particularly important in nuclear reactors since the temperature of the fuel is directly dependent on the effectiveness of heat transfer processes in the reactor core. Heat transfer effectiveness is noticeably reduced when the critical heat flux (CHF) is reached. This causes a large increase in the surface temperature in order to maintain the same level of energy exchange between the heated surface and coolant. CHF is reached when liquid coolant no longer makes contact with the heated surface because the heat flux is sufficiently high for a given set of operating conditions.

Many experimental studies have contributed to the development of a multitude of correlations and models. The database of steady-state CHF data for the widely used CHF look-up table (LUT) contains over 30 000 unique data points [1]. Some researchers have identified parametric regions where more experimental data could increase confidence in existing models, namely at low to medium pressures, extremely high mass fluxes, very high subcoolings, and for small diameter tubes [2] [3]. Still less experimental data is available for CHF during power, flow or pressure transients as may occur during a nuclear reactor accident [4]. Very few experiments have been performed during transients of more than one variable [5].

For these reasons an experimental facility has been constructed at McMaster University to collect CHF data at low to medium pressures of 0.5 to 2.0 MPa at steady state and during power, flow, and/or pressure transients. The purpose of the simulations discussed in this paper is to establish limits on the experimental ranges for pressure, flow, and power to ensure that the test section is not damaged.

2. Background

Heat transfer in convective boiling is governed by several processes whose relative contributions change depending on the conditions in the system. This includes but is not limited to the flow regime, heat flux, mass flux, and local thermodynamic conditions [6]. In general all heat transfer correlations are based on the calculation of a heat transfer coefficient, h, as in Newton's law of cooling:

$$\ddot{q} = h(T_w - T_b)$$

In the above equation, $\ddot{q}$ is the heat flux in W m^{-2}, h is the heat transfer coefficient in W m^{-2} K, and T is the temperature in K. The correlations used to calculate hydrodynamic conditions—including flow regimes—and heat transfer coefficients in RELAP5/SCDAPSIM MOD 3.4 are outlined below.

RELAP5 uses the Chen correlation for flow boiling in the bubbly, slug/churn, and annular mist flow regimes [7]. When using this correlation heat transfer is assumed to be governed by two processes: a 'macroscopic' turbulent convection component, and a 'microscopic' nucleate boiling component. The overall heat transfer coefficient is the sum of the heat transfer components from convection and nucleate boiling [8].

$$h = h_{mac} + h_{mic}$$

The convective contribution is calculated using the Dittus-Boelter correlation and multiplying it by the ratio of the two-phase Reynolds number and the liquid Reynolds number, F. The nucleate boiling contribution is determined by the product of the heat transfer coefficient calculated using the Forster-Zuber correlation and multiplying it by a suppression factor, S, that corrects for the 'effective' wall superheat. The correction factors were derived from experimental data and represented graphically in the original correlation; RELAP5 uses a functional expression derived later to calculate S and F [7].

The Chen, Ozkaynak, and Sundaram correlation for post-dryout heat transfer is used by RELAP5 to calculate heat transfer coefficients during transition boiling in the mist flow regime [7]. This model takes into consideration the effect of vapour superheating due to thermodynamic non-equilibrium. It is assumed that for large wall superheats ($\geq \sim 100°\mathrm{C}$) heat transfer from the wall directly to liquid droplets is negligible. The heat transfer coefficient is determined using a momentum transfer analogy. The ratio of 'actual' thermodynamic quality to equilibrium quality is expressed as an empirical function of dimensionless temperature—the ratio of vapour superheat to the driving superheat—and pressure [9].

Finally, a modified form of the Bromley correlation is used to calculate film boiling heat transfer in the mist flow regime [10]. Bromley modeled film boiling heat transfer as the sum of a conduction component through the vapour film plus a radiation component from the heated surface to the liquid. The original correlation was verified using data from pool boiling experiments in organic liquids [11].

Critical heat flux (CHF) is predicted using Groeneveld *et al*'s 1986 CHF look-up table (LUT) [10]. The 1986 CHF-LUT is based on a database of over 15 000 experimental data points. The CHF-LUT expresses CHF for 8 mm vertical tubes as a function of pressure, mass flux, and local quality in table format. Correction factors are given to adjust table data to other geometries. For example the correction factor for tubes with diameters from 2 to 16 mm is calculated as the ratio of the LUT diameter (8 mm) to the desired diameter to the 1/3 power [12].

RELAP5 determines local hydrodynamic conditions using a one-dimensional two-fluid numerical model of the mass, momentum, and energy conservation equations [10]. Pre-CHF flow regimes are determined using data from the numerical model and the flow regime map of Ishii and Mishima [7]. For subcooled and saturated boiling heat transfer the Chen correlation is used. Once CHF is reached RELAP5 calculates both the transition boiling and film boiling heat transfer coefficients and the greater of the two is used. These are calculated using the Chen, Ozkaynak, and Sundaram correlation for post-dryout (PDO) heat transfer and the Bromley correlation, respectively [10].

In addition to two-phase convective heat transfer, conduction heat transfer in the solid parts of heated components is modeled in one-dimensional radial co-ordinates according to Fourier's law of conduction:

$$\ddot{q} = -k(T)\,\frac{\partial T}{\partial r}$$

Where k is the thermal conductivity in W m^{-1} K. A finite-difference method is used to solve the equation shown above. Axial conduction can be modeled by RELAP5 when the reflood option is used but was not implemented in the model discussed in this paper [10].

3. Simulation Model

The test section at the McMaster University CHF facility is a vertical 6.35 mm Inconel 600 tube with an interior diameter of 4.57 mm. Its heated length is 1 m and it has an inlet development length of at least 0.5 m. This component was modeled using two PIPE components [13] divided into 40 and 20 equal 0.025 m volumes for the heated and unheated sections, respectively, to allow RELAP5 to numerically solve for the local hydrodynamic conditions. The unheated and heated portions were joined by a SNGLJUN 'passive' junction component [13].

A heat structure component was used to model the electrically heated portion of the test section. The heat structure was again divided into 40 equal components. Each component was coupled to the corresponding volume in the heated portion of the test section. The heat structures are modeled as a cylindrical shell with 5 numerical mesh points bounding 4 regions where material properties are calculated. Power was specified to be generated uniformly throughout the 4 regions.

Inconel 600 thermal conductivity as a function of temperature was determined using an exponential expression given by Novog, Yin, and Chang [14]. It should be noted that the expression is only valid up to 773.15 K but was used up to 1273.15 in this model. Therefore temperature distributions within the heated wall at temperatures exceeding this value should be regarded as approximations at best.

Hydrodynamic boundary conditions for the test section were set by specifying the inlet temperature and outlet pressure using time dependent volume components, TMDPVOL. Inlet mass flux was specified using a time dependent junction component, TMDPJUN, that joined the inlet boundary volume to the test section's development length. A SNGLJUN junction joined the test section outlet to the outlet boundary volume.

4. Test Parameters

The following boundary conditions were used during steady-state simulations:

P_o = 0.5, 1.0, 2.0 MPa
G = 500, 1000, 2000 kg m^{-2} s^{-1}
X_i = -0.2, 0.0

Where P_o is the outlet pressure, G is the mass flux, and X_i is the thermodynamic equilibrium quality at the inlet based on the outlet pressure. Simulations using X_i = -0.2 were only run for G = 500 kg m^{-2} s^{-1} and were not used at all during the transient simulations outlined below.

The model was initialized and allowed to reach steady state by first running for 40 s of simulated time using a maximum time step of 10^{-4} s and then allowed to run for an additional 2000 s of simulated time with a maximum time step of 10^{-1} s. After 2040 s of simulated time it was assumed that the model had reached steady state. Steady state data were found by iteratively running the model with different inlet heat fluxes until the 40th discrete volume—the effective 'outlet' of the test section—just reached the transition boiling heat transfer mode. CHF values were determined to within 10 kW m^{-2}.

Rate	**10**		**20**		**50**		**100**	
G	Initial	Final	Initial	Final	Initial	Final	Initial	Final
500	600	200	700	200	1000	200	1500	200
1000	1100	500	1200	500	1500	500	2000	500
2000	2100	1000	2200	1000	2500	1000	3000	100

Table 1: Initial and final mass fluxes for transients with rates shown in the top row and steady-state reference mass fluxes in the leftmost column. Units are in kg m^{-2} s^{-1} for mass fluxes and kg m^{-2} s^{-2} for rates.

Transient data were taken for flow reduction ramps of 10, 20, 50, and 100 kg m^{-2} s^{-2}. The test matrix for initial and final inlet mass fluxes for each of the transients is shown in Table 1. The initial and final flow rates were chosen independently of pressure. For each transient simulation the model was allowed to reach steady-state over 2040 s using the initial mass flux shown in Table 1. Steady-state CHF was used as the heat flux throughout the initialization and transient.

5. Results & Discussion

Steady state heat transfer results are shown in Figures 1-4. It appears from the heat transfer data that the wall superheat is consistent for each of the mass fluxes as a function of pressure for the hydrodynamic conditions in these simulations. The wall temperatures at different pressures differ by roughly constant amounts. This can be attributed to the difference in saturation temperature which increases with pressure.

The fluid at the inlet is subcooled since the inlet temperature is at saturation according to the outlet conditions and the pressure drop is non-zero. This is shown in some simulations by the axial increase in wall temperature near the inlet corresponding to the fluid temperature rising until it reaches the local saturation temperature. This effect is most evident for subcooled inlet conditions but can also be seen in the high mass flux simulation results since the pressure drop is relatively large. Wall temperature then axially decreases once the bulk fluid reaches the saturation temperature at the local pressure. The axial wall temperature decrease is consistent with the local pressure and corresponding saturation temperature once the fluid is saturated.

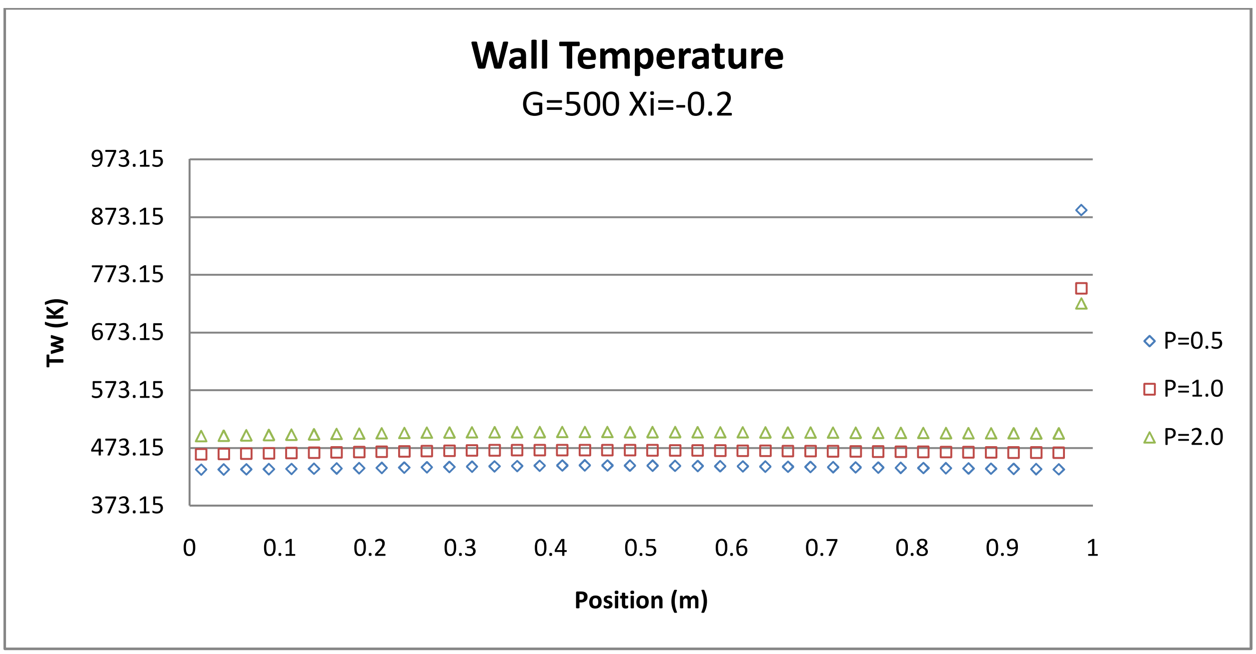

Figure 1: Axial wall temperature for G = 500 kg m^{-2} s^{-1} and subcooled inlet conditions. Pressure, P, is in MPa.

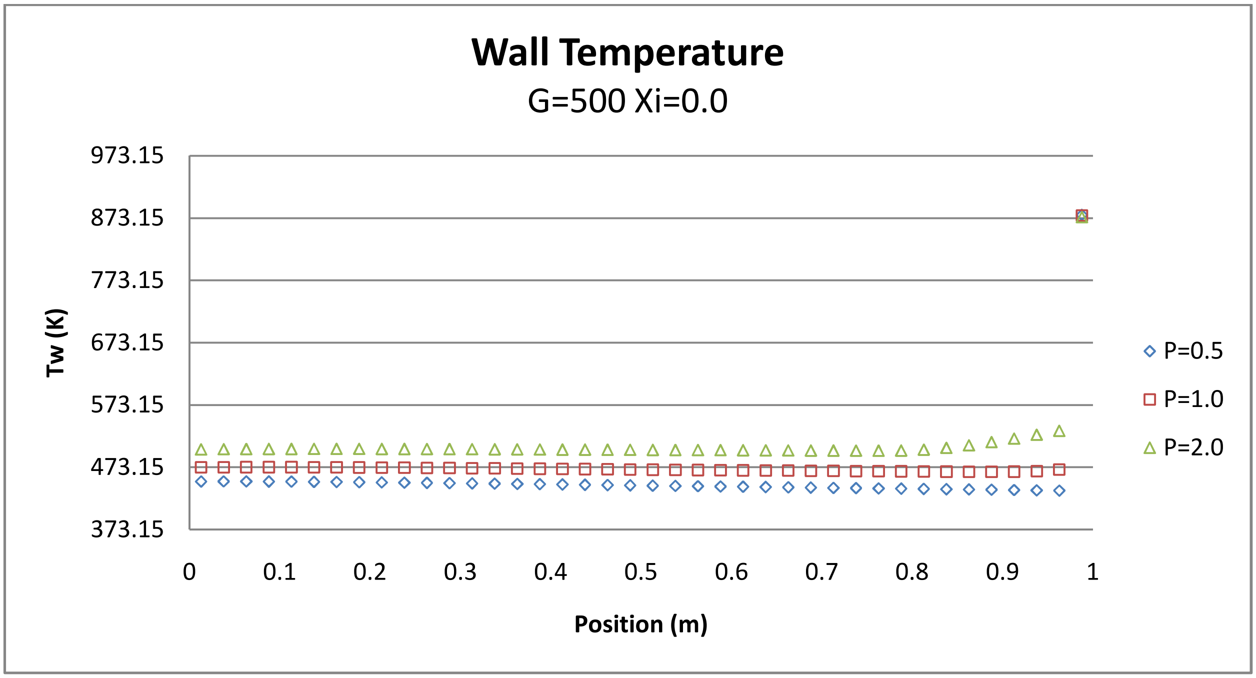

Figure 2: Axial wall temperature for G = 500 kg m^{-2} s^{-1} and saturated inlet conditions. Pressure, P, is in MPa.

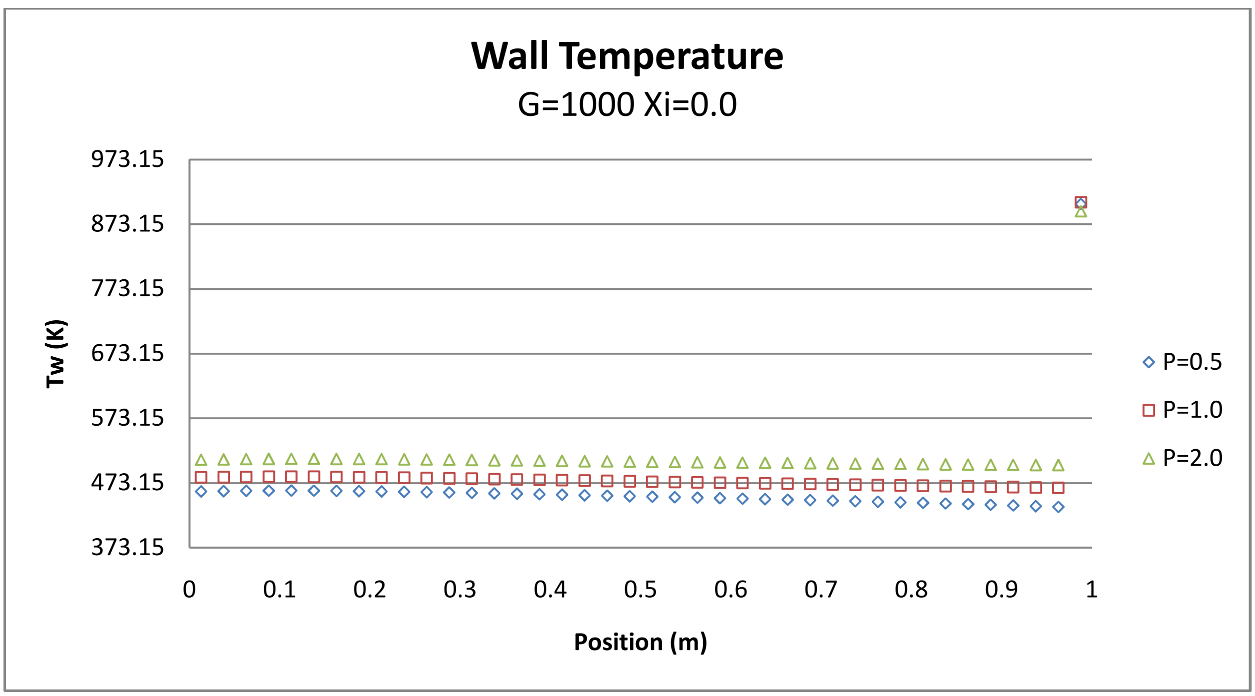

Figure 3: Axial wall temperature for G = 1000 kg m^{-2} s^{-1} and saturated inlet conditions. Pressure, P, is in MPa.

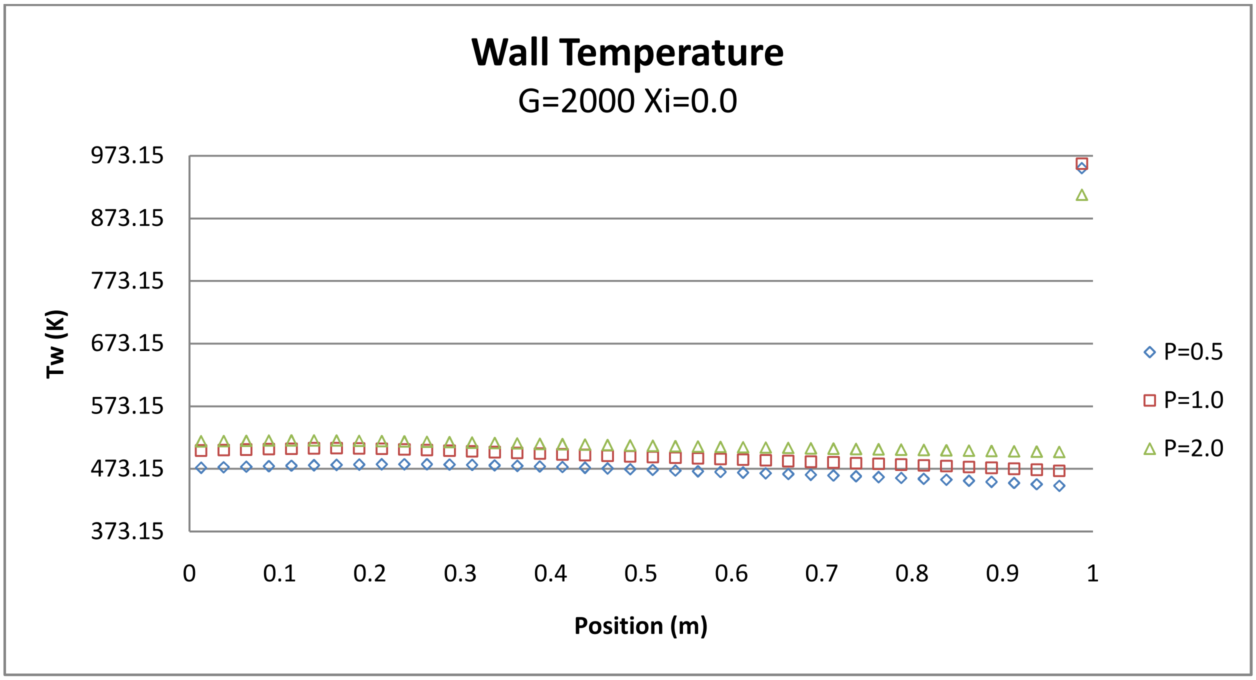

Figure 4: Axial wall temperature for G = 2000 kg m^{-2} s^{-1} and saturated inlet conditions. Pressure, P, is in MPa.

CHF data and a summary of the outlet temperatures at CHF are shown in Figure 5 and Figure 6. It is evident from the heat transfer data that the wall temperature at CHF increases with the mass flux for all pressures. CHF increases with pressure for mass fluxes of 500 and 1000 kg m^{-2} s^{-1} but increases between 0.5 and 1.0 MPa and is less at 2.0 MPa for the simulations with G = 2000 kg m^{-2} s^{-1}. This indicates that for the model used in RELAP5 the wall temperature at CHF is independent of the heat flux contrary to what is intuitive.

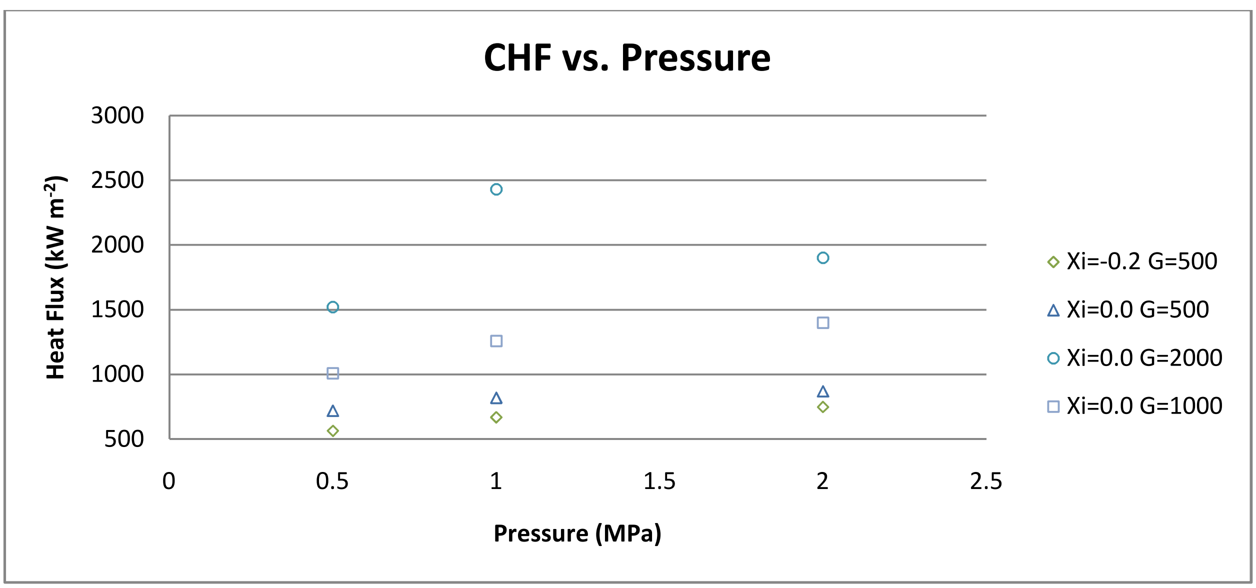

Figure 5: CHF data as a function of pressure. Mass flux, G, is in kg m^{-2} s^{-1}.

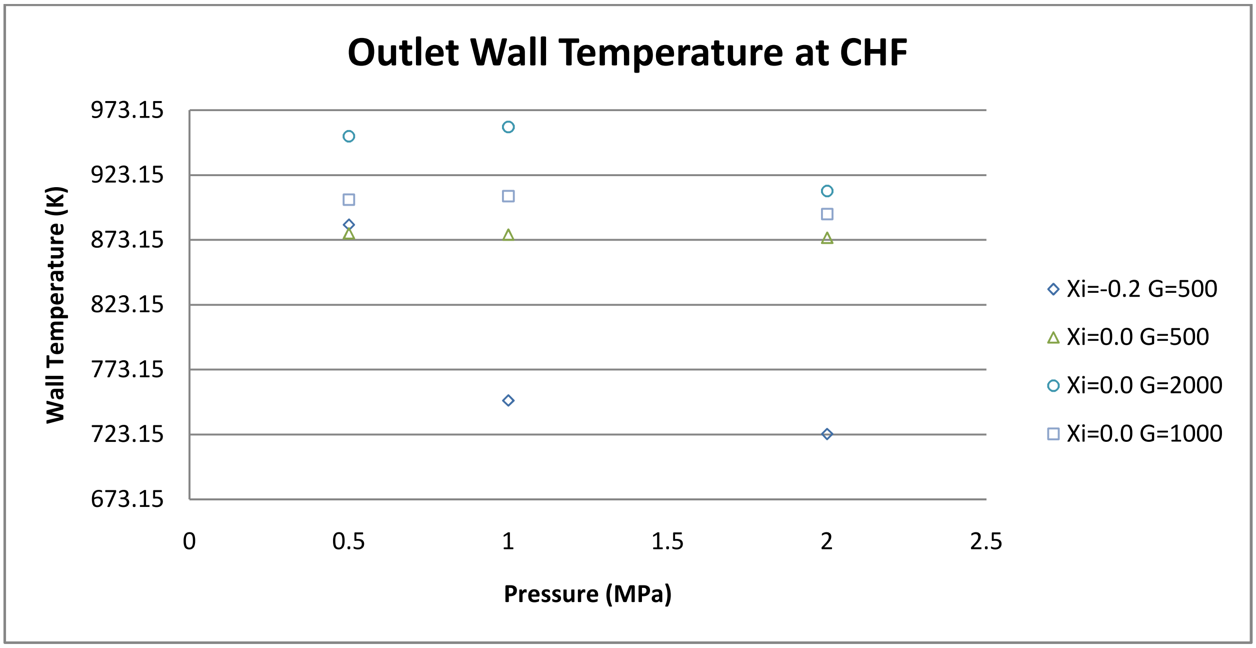

Figure 6: Outlet wall temperature at CHF as a function of pressure. Mass flux, G, is in kg m^{-2} s^{-1}.

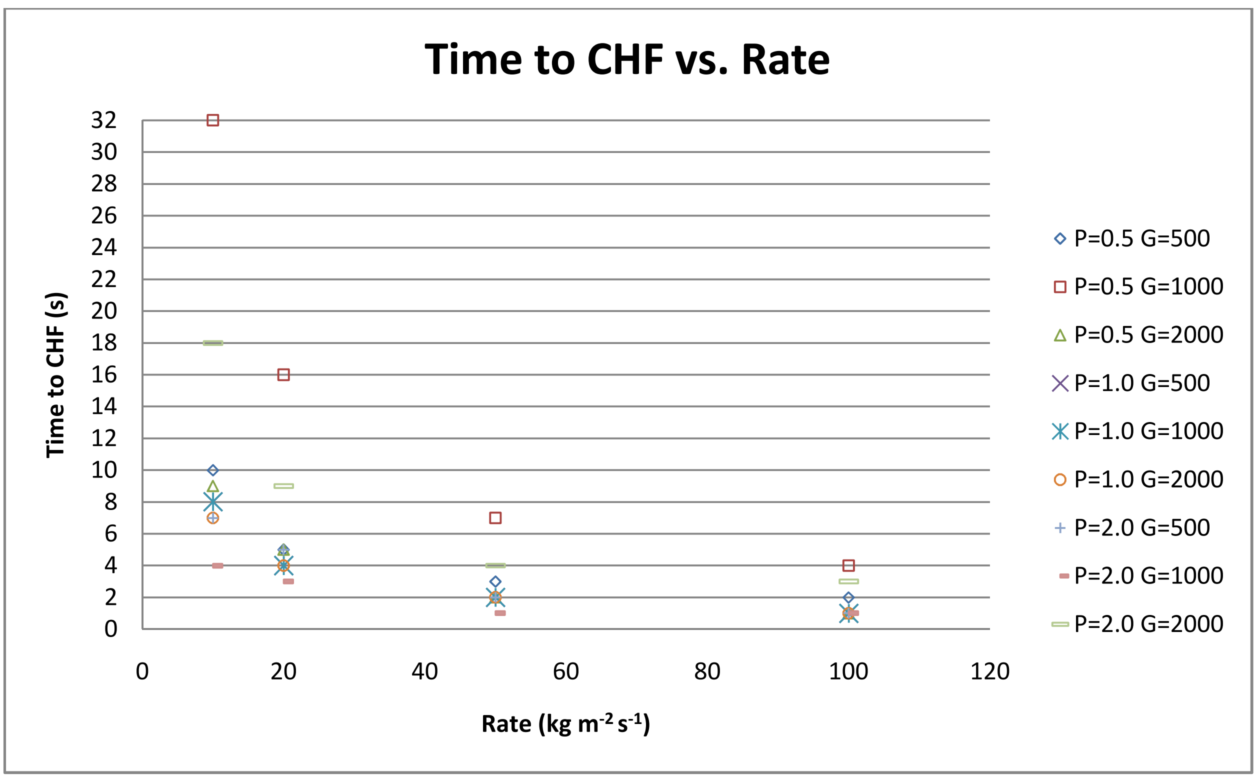

Figure 7: Time to reach CHF vs. rate. Pressure, P, in MPa, and mass flux, G, in kg m^{-2} s^{-1}. CHF times were determined with a resolution of 1 s.

The heat transfer data were taken at the point where CHF is reached at the outlet. As discussed above the wall superheats are nominally constant for the given inlet conditions (mass flux and subcooling). This indicates that for the correlations and models used in RELAP5 the CHF is roughly proportional to the heat transfer coefficient for these temperatures and pressures. This holds true even for the case where the CHF does not show a consistent trend with pressure—when $G = 2000 \text{ kg m}^{-2} \text{ s}^{-1}$.

Transient results are shown as a function of ramp flow rate decrease in Figure 7. In all cases the time to reach CHF is inversely proportional to the rate of decrease. This indicates that, to within the 1 s resolution used to output the simulation data, the inlet mass fluxes at CHF were nominally independent of the rate of flow decrease. This could be due to the fact that the liquid and vapour velocities, according to the RELAP5 models and correlations, are very high and have a very short 'residence' time in the heated test section. Therefore the conditions at the outlet responded very rapidly to the conditions at the inlet. These observations are consistent with the use of the local conditions formulation of the CHF-LUT, based on steady-state data, to determine CHF during transients.

6. Conclusion

RELAP5/SCDAPSIM MOD 3.4 will be useful for predicting the results of experiments at the McMaster University CHF facility including but not limited to wall temperatures at CHF. This will allow the experiment users to determine the likelihood of damaging the test section. In addition it will allow heat transfer data gathered at the facility to be directly compared with widely used heat transfer correlations such as the Chen correlations for convective boiling and PDO heat transfer. This is especially useful because even if 'predictive' simulations are run before experiments are conducted it may not always be possible to exactly control the mass flux or inlet temperature—especially during transient cases. It will then be possible to run simulations using the 'real' experimental boundary conditions for direct comparison.

The CHF-LUT used by RELAP5 has been updated twice since it was implemented in the code. Experiments will be performed to compare the accuracy of RELAP5's CHF predictions based on the 1986 CHF-LUT to real experimental data, as well as the updated 2006 CHF-LUT [1] and other models and correlations.

The CHF facility is capable of following not only flow transients but also power and pressure transients. Future work will include simulations and experiments incorporating all of these types of transients.

7. References

[1] Groeneveld, D.C., Shan, J.Q., Vasić, A.Z., Leung, L.K.H., Durmayaz, A., Yang, J., Cheng, S.C., and Tanase, A. "The 2006 CHF look-up table," *Nuclear Engineering and Design,* No. 237, 2007, pp. 1909-1922.

[2] Olekhnovitch, A., Teyssedou, A., Tapucu, A., Champagne, P., and Groeneveld, D.C. "Critical heat flux in a vertical tube and low and medium pressures: Part I. Experimental results," *Nuclear Engineering and Design,* No. 193, 1999, pp. 73-89.

[3] Hall, D.D., Mudawar, I. "Critical heat flux (CHF) for water flow in tubes—I. Compilation and assessment of world CHF data," *International Journal of Heat and Mass Transfer,* No. 43, 2000, pp. 2573-2604.

[4] Kataoka, I., and Serizawa, A. "Transient boiling heat transfer under forced convection" in Handbook of Heat and Mass Transfer, Cheremisinoff, N.P., ed., Gulf Publishing, 1986, pp. 327-403.

[5] Celata, G.P., Cumo, M., D'Annibale, F., Farello, G.E., and Mariani, A. "CHF behavior during pressure, power and/or flow rate simultaneous variations," *International Journal of Heat and Mass Transfer,* Vol. 34, Iss. 3, 1991, pp. 723-738.

[6] Collier, J.G., and Thome, J.R. Convective boiling and condensation, 3rd ed., Oxford University Press, 1996.

[7] RELAP5/MOD3.3 Code manual volume IV: Models and correlations. Nuclear safety analysis division, Information systems laboratories, Inc., NUREG/CR-5535/Rev 1-Vol IV, 2001.

[8] Chen, J.C. "Correlation for boiling heat transfer to saturated fluids in convective flow," *Industrial and Engineering Chemistry Process Design and Development,* Vol. 5, Iss. 3, 1966, pp. 322-329.

[9] Chen, J.C., Ozkaynak, F.T., and Sundaram, R.K. "Vapor heat transfer in the post-CHF region including the effect of thermodynamic non-equilibrium," *Nuclear Engineering and Design,* No. 51, 1979, pp. 143-155.

[10] RELAP5/MOD3.3 Code manual volume I: Code structure, system models, and solution methods. Nuclear safety analysis division, Information systems laboratories, Inc., NUREG/CR-5535/Rev 1-Vol I, 2001.

[11] Bromley, L.A. "Heat transfer in stable film boiling," *Chemical Engineering Progress,* Vol. 46, Iss. 5, 1950, pp. 221-227.

[12] Groeneveld, D.C., Cheng, S.C., and Doan, T. "1986 AECL-UO critical heat flux lookup table," *Heat Transfer Engineering,* Vol. 7, Iss. 1-2, 1986, pp. 46-62.

[13] The RELAP5-3D code development team. RELAP5-3D© code manual volume 2, Appendix A: RELAP5-3D© input data requirements, v 2.4. Idaho National Laboratories, INEEL-EXT-98-00834-V2. Accessed April 6, 2009. Available: http://www.inl.gov/relap5/r5manuals/ver_2_4/vol2_app_a_v2_4.pdf

[14] Novog, D.R., Yin, S.T., and Chang, J.S. "Recent advances in high heat flux smooth and swirl flow boiling of water," *Fusion Science and Technology,* Vol. 52, Iss. 4, 2007, pp. 880-884.